

# Experimental Performance Analysis of Digital Beam Forming on Synthetic Aperture Radar

Junghyo Kim, Denis Becker, Werner Wiesbeck  
Institut für Höchstfrequenztechnik und Elektronik, Universität Karlsruhe, Germany

Marwan Younis  
German Aerospace Center, Microwaves and Radar Institute, Germany

## Abstract

In this paper, we present the experimental results of a Digital Beam Forming (DBF) Synthetic Aperture Radar (SAR) performance on the purpose of the High-Resolution Wide-Swath (HRWS) SAR concept. A ground-based SAR system successfully demonstrates the DBF SAR operation. The demonstrator acquired SAR raw data with very dense spatial sampling rate in order to obtain various sampling rates. We evaluate DBF performance with respect to the image quality factor with two different types of the beam former, a fixed-beam former and an adaptive beam former. The results show that an adaptive DBF algorithm offers a wide range of the selection of the pulse repetition frequency (PRF). In addition we evaluate the noise performance compared to a reference mono-static SAR system on the same condition on single target experiment.

## 1 Introduction

A spaceborne SAR system is used in the wide spectrum of the remote sensing owing to its wide-area observation capability and high resolution. A modern SAR system based on the phased-array antennas realizes the multiple SAR operation such as the stripmap, spotlight and scan mode operation. However, this system does not fulfill the users demands for SAR data for a wide area with the fine resolution since there is a fundamental trade-off between the ambiguity and the swath width. Additionally, the lifetime of a satellite depends on the fuel budget to maintain its orbit and motion control. A SAR sensor observing the wide area can reduce the revisit time and thereby extend the operation period. Therefore, the simultaneous achievement of the wide coverage and fine spatial resolution is quite attractive not only for the SAR users, but also in the system point of view. Such a simultaneous observation of a wide area with fine resolution provides the useful information, especially for the dynamic target surveillance of oceans, ice and artificial moving targets. On a bi- or multi-static configuration this fundamental restriction can be resolved by introducing an appropriate DBF technique. The HRWS SAR concept exploits the smart antenna technique on 2 dimensional array antenna constellation in order to compensate the azimuth ambiguity resulting from reduced PRF. In this paper we focus on the DBF SAR performance in azimuth directio. Several DBF algorithms were proposed with respect to a spectral estimation in spatial frequency domain[1],[2],[3]. In this paper, we introduce the experimental results through a simplified 2-dimensional measurement. Numerous array configurations

are feasible for the experiment. Nevertheless, the preliminary experiment contributes to the evaluation of a uniform linear array (ULA) DBF SAR as shown in figure 1.

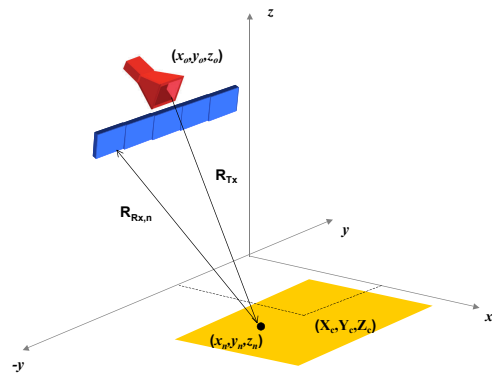


**Figure 1:** Geometry of a DBF SAR with an uniform linear array on the receive

## 2 Digital Beam Forming on SAR

The performance of a DBF SAR significantly relies on the quality of filtering the desired Doppler component and suppressing the neighboring replica of Doppler spectrum caused by lower PRF than Nyquist sampling criterion. At an arbitrary frequency  $\omega_o$  bin, the obtained baseband Doppler spectrum  $S_l$  by  $l$ th antenna is basically given by

the superposition of the baseband spectrum and its replicas.

$$S_l = \sum_{\alpha=-\infty}^{\infty} S_l(\omega_o, k_a + \alpha k_s) \cdot \Omega_D \quad (1)$$

where  $\alpha$  is an integer ( $0, \pm 1, \pm 2, \dots$ ) standing for the order of the spectrum replicas. The baseband spectrum is only visible within the rectangular window  $\Omega_D \in [-\frac{k_s}{2}, \frac{k_s}{2}]$  after Fourier transform.  $k_a$  and  $k_s$  are the Doppler spatial frequency and spatial sampling frequency, respectively. Multiple orthogonal beams generated by a DBF processor decompose this aliased Doppler spectrum into the angular Doppler spectrum domain  $\theta_d$ , which is defined by

$$\theta_d = \arcsin \frac{k_a + \alpha k_s}{2k} \approx \frac{k_a + \alpha k_s}{2k} \quad (2)$$

$k$  denotes the wave number. A post processing following the DBF reconstructs the desired full Doppler spectrum. Consequently it leads to increase the number of samples in azimuth and avoid an ambiguity in SAR image due to spatial under-sampling. From (2), the steering vector  $\mathbf{a}_\alpha$  in the angular Doppler domain is given by

$$\mathbf{a}_\alpha = [a_0, a_1, \dots, a_{N_r-1}]^T \quad (3)$$

$N_r$  is the number of the receive antenna. It must be noted that the DBF on SAR generates  $N_r$  beams, so that the steering vector becomes  $N_r$ -by- $N_r$  matrix. The total steering matrix  $\mathbf{A}$  is described by

$$\mathbf{A} = [\mathbf{a}_0, \mathbf{a}_1, \dots, \mathbf{a}_{N_r-1}] \quad (4)$$

Substituting the steering matrix into the weight matrix  $\mathbf{W}$ , a fixed beam former output  $\mathbf{Y}$  is given by

$$\mathbf{Y} = \mathbf{W}^H \mathbf{S} \quad (5)$$

As a high resolution beam former, Minimum Variance Distortionless Response (MVDR) method, which is well known as Capon's beam former, provides better performance on the condition of non-uniform spatial sampling[3]. The weight matrix is

$$\mathbf{W}_{Capon} = \frac{\mathbf{R}^{-1} \mathbf{A}(\theta_d)}{\mathbf{A}^H(\theta_d) \mathbf{R}^{-1} \mathbf{A}(\theta_d)} \quad (6)$$

From the filter theory an adaptive beam former has been derived in [1]. All receive subarrays have unique transfer function, which contains the antenna characteristics and the delay information from target to the individual receive antenna. The estimated transfer function from the antenna geometry plays role as a reconstruction filter. The reconstruction filter is an inverse of the transfer function[1] and is equivalent to the inverse of the steering matrix.

$$\mathbf{W}_{Recon}^H = \mathbf{H}^{-1} = \mathbf{A}^{-1} \quad (7)$$

In next section we introduce the ground-based experiment and the following section we evaluate the performance of the digital beam formers above.

### 3 GB Experiment of DBF SAR

The measurement will be performed with the ground-based SAR system at X-band ( $f_c = 9.65$  GHz) with 300MHz system bandwidth. The demonstration system is composed of the antenna subsystem, Radio Frequency (RF) subsystem, and the platform block.

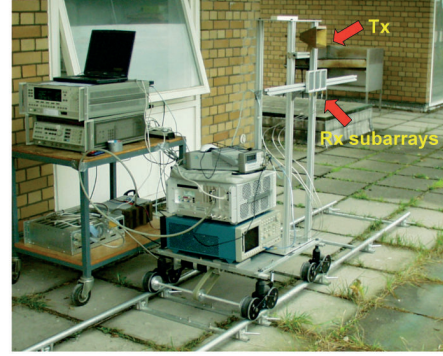


**Figure 2:** The implemented GB DBF SAR demonstrator under test

The implemented demonstrator contributes a single target measurement in order to verify the idea of DBF for the HRWS SAR concept and system studies. A ULA with three receive subarrays are adapted and are vertically separated with 23 cm on purpose of avoiding coupling from the transmit antenna. The length of the receive subarray is 6.8 cm, which yields total length of 20.4 cm. It should be noted that, in uniform sampling scenario, the separation between the effective phase centers corresponds to the half of the subarray length. Hence the uniform spatial sampling fully depends on the antenna size [4], For the optimum sampling step movement of the platform must be 10.2 cm. However, we evaluate the DBF SAR performance for various spatial sampling distance  $\Delta d$ , which means that the spatial sampling distance, which changes from 1.02 cm to 10.2 cm as shown in figure 3.

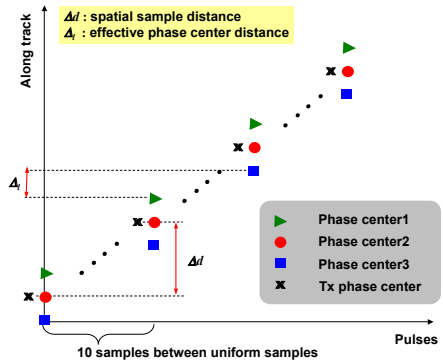


**Figure 3:** The spatial sampli in the GB exeriment using 3 ULA

## 4 DBF SAR Performance

The obtained SAR data with DBF SAR operation is used to reconstruct the single point target response. The  $\omega - k$  SAR processing is employed for the image reconstruction.

### 4.1 Channel Imbalance Effect

Prior to applying DBF on the raw data, the array system must be carefully calibrated. The former research shows that the channel imbalance causes a high frequency sinusoidal error. The critical point is the fact that the sinusoidal phase error have an identical frequency to PRF. This phase error hence causes unexpected spectral overlapping between original spectrum and shifted spectrum caused by the convolution relation in spatial Doppler domain. Usually array phase error can be easily corrected by the array calibration on the ground. However, the channel imbalance that occurs during the operation in the extreme environment(space) should be considered in practice. Figure 4 shows the distorted target response by the high ambiguities that are generated by the channel imbalance.

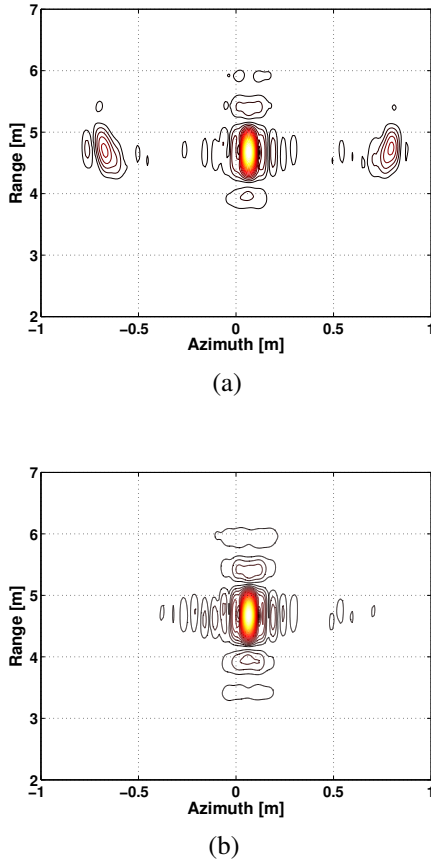


**Figure 4:** The reconstructed DBF SAR image (a) with the channel imbalance condition (b) after calibration

### 4.2 Non-Uniform Sampling Effect

After the array calibration we applied several DBF algorithms stated in previous section and reconstructed the point target response with various PRF. We define the over-sampling ratio with respect to the optimum uniform sampling distance. In this experiment the uniform sampling distance is 10.2cm. If this optimum sampling distance is not fulfilled, then the raw data is acquired with non-uniform sampling in the azimuth. In principle the non-uniform sampling in the DBF SAR brings the same effect as the channel imbalance. However, it will be shown that the MVDR method and the reconstruction filter method provide the stable performance under the non-uniform condition.

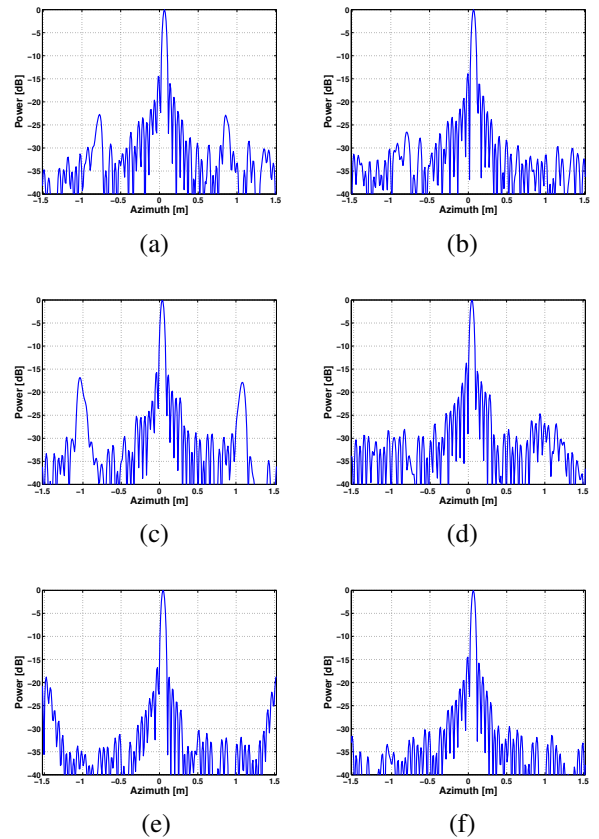


**Figure 5:** The reconstructed azimuth profile with various over-sampling ratio, 10%, 30% and 50% from the top. (a),(c),(e) are for a fixed beam former and (b),(d),(f) for Capon's beam former

As shown in the right column of figure 5, the Capon's beam former provides the steady ambiguity suppression compared to the conventional fixed beam former in the same condition. We don't present the results of the reconstruction algorithm in [1] since the reconstruction filter algorithm shows an analogue of MVDR as investigated in [5]. Remarkable feature is the fact that the adaptive beam former, such as MVDR and reconstruction filter algorithm, adjust the beam forming gain for the purpose of

the adaptive nulling in non-uniform sampling. Thus the ideal Signal-to-Noise Ratio (SNR) is not achievable. It must be emphasized that the maximum sampling distance for a conventional monostatic SAR is 3.4cm in this case. In the following section we analyze the more detail.

## 5 Analysis

The reconstructed point target response is evaluated for the various sampling rate (PRF) as introduced in previous section. Here we evaluate the Azimuth Ambiguity Suppression Ratio (AASR) of the two beam formers. The two-way antenna pattern performs an amplitude tapering, so that the ambiguity becomes a peak side lobe under the non-uniform sampling.

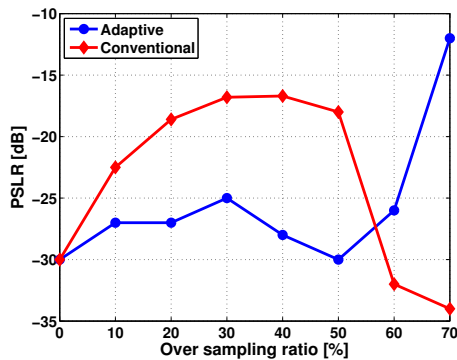


**Figure 6:** The measured Peak to Side Lobe Ratio with the over-sampling ratio

It is obvious that the Capon's beam former shows the stable suppression property compared to the fixed beam former. In the higher over-sampling region around 66% a break-out point exists. The reconstruction filter algorithm and Capon's algorithm take a matrix inverse to defined the weight matrix. Around the break-out point the covariance matrix becomes singular due to the coincident spatial samples. Thus a proper weight matrix can not be defined. In contrast to the adaptive beam former, the fixed beam former has a its iterative null point at this point. So the performance becomes similar to the uniform sampling case with this sampling ratio. These results can be observed in the Integrated Side Lobe Ratio( ISLR) as well. Although it doesn't show the pure noise performance of only the beam former, the ISLR reflects the estimated noise performance of the DBF SAR. As shown above the non-uniform sampling affects the total noise on the SAR image in case of the conventional beam former compared to the image from the adaptive beam former. At the break point the ISLR of the adaptive beam former degrade significantly due to the same effect stated above.

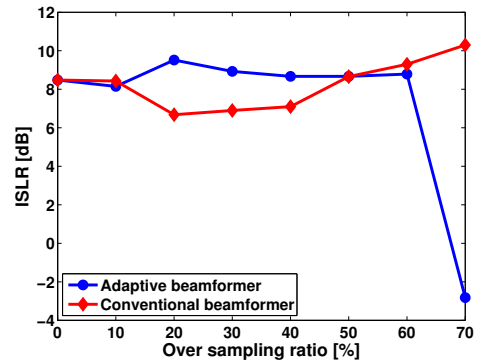


**Figure 7:** The measured Integrated Side Lobe Ratio with the over-sampling ratio

## 6 Conclusion

Using a ground-based SAR system we evaluate the proposed DBF performance for SAR application. It is obviously demonstrated that the DBF SAR allows increasing the swath width and provides the performance improvement. In practice, we could observe the fact that an accurate array calibration is necessary to achieve the optimum performance. The effect of systematic phase and amplitude error is servere because it contributes unexpected spectral overlapping. From the various spatial sampling experiments we showed that the adaptive beamformer has tolerance to select the wide range of PRF. However, it is emphasized that the adaptive beam former fully dependent to the SNR of the input signal and calibration accuracy. Therefore an optimization strategy in practical system design will be studied in future work.

## References

- [1] G. Krieger, N. Gebert, A. Moreira: *Unambiguous SAR Signal Reconstruction from Non-Uniform Displaced Phase Centre Sampling*, IEEE GRS Letters, Vol. 1, No. 4, Oct. 2004, pp. 260-264.
- [2] M. Younis: *Digital Beamforming for High Resolution Wide Swath Real and Synthetic Aperture Radar*, Ph.D. Dissertation, IHE, Universität Karlsruhe, 2004.
- [3] Z. Li, H. Wang, Z. Bao: *Generation of Wide-Swath and High-Resolution SAR Images from Multichannel Small Spaceborne SAR System*, IEEE GRS Letters, Vol. 2, No. 1, Jan. 2005, pp. 82-86.
- [4] M. Younis, C. Fisher, W. Wiesbeck: *Digital Beam Forming in SAR System*, IEEE Transaction GRS, Vol. 41, No. 71, Jul. 2003, pp. 1735-1739.
- [5] N. Gebert, G. Krieger, A. Moreira: *Digital Beam Forming for HRWS-SAR Imaging: System Design, Performance, and Optimization Strategies*, IEEE Proceeding IGARSS, Jul. 2006, pp. 1836-1839.